Integral and differential cross section measurements at low collision energies for the $N_2^+ + CH_4/CD_4$ reactions

Christophe Nicolas[a)]
Department of Physics, Technische Universität Chemnitz, 09107 Chemnitz, Germany, and Laboratoire de Chimie Physique, Bâtiment 350, Centre Universitaire Paris-sud, 91405 Orsay Cedex, France

Raquel Torrents and Dieter Gerlich
Department of Physics, Technische Universität Chemnitz, 09107 Chemnitz, Germany

(Received 24 May 2002; accepted 14 November 2002)

Absolute integral cross sections are measured in the collision energy range between 0.1 to 3.5 eV for the $N_2^+ + CH_4$ and $N_2^+ + CD_4$ reactions using the universal guided ion beam apparatus. The reaction branching ratio, $CX_3^+ : CX_2^+ : N_2X^+$ (X=H or D), is found to be 0.86:0.09:0.05 and 0.88:0.07:0.05 for the $N_2^+ + CH_4$ and $N_2^+ + CD_4$ reactions, respectively. The CH_3^+/CH_2^+ ratio is constant over the whole collision energy range and very similar to the one obtained for the almost isoenergetic $Ar^+ + CH_4$ reaction. Axial velocity distributions of the product ions are measured by time of flight at collision energies between 0.1 and 3.5 eV. The results provide direct insight into the reaction dynamics. The dissociative charge transfer channels, leading to CH_3^+ and CH_2^+ product ions, occur via an electron jump combined with some exchange of momentum between the colliding partners. The H (D) transfer leading to N_2H^+ can be described as a direct process, similar to a spectator stripping mechanism. Various isotope effects are observed, the dominant being that the cross sections for reaction with CH_4 are up to 20% bigger than the corresponding ones for CD_4.
 [DOI: 10.1063/1.1535423]

I. INTRODUCTION

Though ion–molecule reaction dynamics have been extensively studied, detailed elementary mechanisms are still not generally understood with the necessary accuracy for detailed models. This is particularly the case for quasiresonant charge transfer reactions, such as the $N_2^+ + CH_4$ reaction. This reaction plays a key role in the Titan ionosphere. Indeed, the largest Saturn satellite atmosphere is mainly composed of $N_2(\approx 95\%)$, $CH_4(\approx 5\%)$ and traces of C_2H_2, C_2H_4 and C_2H_6.[1] The reaction between N_2^+ and CH_4 is the primary step of the general reaction pathway leading to the formation of H_2CN^+ ions, the most abundant ionic species according to Keller *et al.*[2] This process is one of the most efficient destruction mechanisms for N_2^+ ions and contributes significantly to the production of CH_3^+ ions. It is therefore very important to precisely measure the product branching ratio. It is also necessary to characterize the internal and translational energy content of the products, since further reactions involving these intermediate product ions can be strongly affected by their energy content. Up to now, ionospheric models only include thermal rate constants for ground state ions, due to the lack of experimental data. A detailed study of one of the most important ion–molecule reactions of the Titan ionosphere is particularly relevant to improve the models, for the determination of realistic ion density profiles.[3] The other more fundamental aim of the present study is to elucidate in detail reaction mechanisms for the different channels, in particular, the dominant channel, dissociative charge transfer.

The different possible reaction channels coming from the reaction of N_2^+ with CH_4 are

$$N_2^+ + CH_4 \rightarrow CH_4^+ + N_2, \qquad \Delta H^\circ = -2.97 \text{ eV} \qquad (1H)$$

$$\rightarrow CH_3^+ + N_2 + H, \qquad \Delta H^\circ = -1.33 \text{ eV} \qquad (2H)$$

$$\rightarrow CH_2^+ + N_2 + H_2, \qquad \Delta H^\circ = -0.48 \text{ eV} \qquad (3H)$$

$$\rightarrow N_2H^+ + CH_3, \qquad \Delta H^\circ = -2.56 \text{ eV}. \qquad (4H)$$

In the following, the letter H or D will be added to the reaction channel in cases where it is necessary to distinguish between reactions with CH_4 and CD_4.

The dominant channel is the (2H) dissociative charge transfer leading to CH_3^+ product ions, the (3H) and (4H) channels are minor and the (1H) nondissociative charge transfer has not been observed.[1] The channels (2H) and (3H), leading to CH_3^+ and CH_2^+ ions, have been previously investigated with ion cyclotron resonance (ICR),[1,4] selected ion flow tube (SIFT),[5,6] and free jet flow reactor techniques.[7] In these studies only thermal rate coefficients were measured. The (4H–D) H or D transfer channels were studied in the 0.1–30 eV collision energy range in crossed beam experiments.[8,9] The forward scattered velocity distribution of the N_2H^+ (or N_2D^+) product ions was measured, clearly indicating a direct H (D) transfer process.

The branching ratio between all channels, i.e., (2H):(3H):(4H), was reported for the first time by McEwan *et al.*[1] to be 0.80:0.05:0.15. However, this branching ratio is

a)Electronic mail: nic@leea.lbl.gov

difficult to measure, as there is a mass overlap between N_2H^+ (mass 29) and the $C_2H_5^+$ ion product (also mass 29) coming from secondary collisions between slow CH_2^+ and CH_3^+ ions and the CH_4 target gas. In the present study, deuterated methane was used to avoid the mass overlap between N_2D^+ (mass 30) and $C_2D_5^+$ (mass 34). This allows precise measurements of the reaction channel branching ratio and unambiguous separation of the contribution of these two ions in the time-of-flight spectra.

For reactions of N_2^+ with both CH_4 and CD_4, absolute integral reaction cross sections are measured as a function of collision energy in the 0.1–3.5 eV range in the center of mass frame (CM). Additional information about reaction dynamics is obtained from differential cross sections. By time-of-flight measurements, the velocity distribution of product ions along the detection axis is obtained. This is made possible through the use of the guided ion beam (GIB) technique. In this paper, after a brief description of the GIB apparatus, the measurement procedures and the data analysis will be explained. Then results of integral and differential cross sections as a function of collision energy will be presented. In the last part, reaction mechanisms will be discussed for the charge transfer and the H (D) transfer channels.

II. EXPERIMENT

The experiments were performed in the universal GIB-apparatus. It has been previously described in detail,[10–13] so only a short description is given here. The N_2^+ primary ions are produced in a radio frequency (rf) storage ion source by electron impact. Primary ions are extracted with a 12–15 μs and 5 V amplitude pulse applied to the exit electrode and injected into a rf quadrupole. The quadrupole is operated in a high-energy-resolution, low pass mass filter mode. The focusing and guiding properties are used for preparing the N_2^+ ions with a kinetic energy spread between 30 and 40 meV. These ions are injected into a first rf octopole device and guided by it into the reaction cell. The parent ion kinetic energy is defined by the dc potential difference between the first octopole and the region which the ions are created in the source.

The reaction of the parent ions with methane takes place in the first octopole in a scattering cell filled with the neutral target gas at a typical pressure of 4×10^{-5} Torr, whose absolute value is measured by a Baratron capacitance manometer.

The product ions are collected with nearly 100% efficiency by the radio frequency guiding field, then guided by a second octopole, mass selected by a 90° deflection magnetic sector analyzer, and are finally detected using a Daly-type detector. The second octopole is typically floated 0.2–0.5 V below the first one in order to avoid the discrimination of slow ions in the transition region between the two octopoles or due to potential distortions in the second octopole. The entrance electrode of the first octopole is pulsed in order to reflect those ions that are backward scattered in the laboratory frame.

From the measurements of the parent and product ion intensities and the absolute pressure of the neutral target gas, reaction cross sections are derived as described below. Neutral gas samples used in the ion source or as reactant were all of analytical purity.

N_2^+ parent ions are produced by electron impact with an electron energy below 16 eV. Only the fundamental electronic state ($X\,^2\Sigma_g^+$) is accessible. With a nitrogen pressure in the source of 10^{-4} Torr and a mean storage time on the order of milliseconds, most ions are relaxed by collisional quenching to their lowest vibrational state $v=0$. The reaction of N_2^+ ions with Ar is used to determine the vibrational relaxation of the primary ions. For calibration, the results of Schultz and Armentrout[14] for the $v=0$ state and of Lindinger *et al.*[15] for the $v=1$ state are used. A fit of the absolute integral cross section by a linear combination of functions describing the cross section for $v=0$ and $v=1$ shows that $98.5\pm0.1\%$ of N_2^+ primary ions are in the ground vibrational state (see Ref. 16 for more details).

III. MEASUREMENT PROCEDURES AND DATA ANALYSIS

A. Absolute integral cross section

For the two systems, absolute integral cross sections are measured as a function of collision energy between 0.1 and 3.5 eV CM. The integral cross sections are corrected for contributions from ^{13}C isotopes. The mode in which the first quadrupole mass filter is operated suppresses all masses above 28 u, i.e., there is no contribution from $^{14}N\,^{15}N^+$ ions. The primary beam attenuation is maintained below 5% during the whole experiment in order to work in a single collision regime. Therefore the integral cross sections can be calculated in good approximation using simply the thin target approximation. The resulting error is negligible compared to systematic uncertainties, which are estimated to be $\pm20\%$.[11] A rather large source of error is due to secondary collisions between backward scattered ions that go slowly through the reaction cell a second time. Secondary reactions of CH_3^+ and CH_2^+ with CH_4 produce $C_2H_5^+$ ions. Due to the high reactivity of CH_3^+ with CH_4 and the fact that CH_3^+ is the major product of the $N_2^+ + CH_4$ reaction, the amount of $C_2H_5^+$ is significant and the results have to be corrected. To correct the $N_2^+ + CD_4$ results for secondary contributions, the part of $C_2D_5^+$ coming from CD_2^+ and CD_3^+ is determined with the $k_{CH_{3+}}/k_{CH_{2+}}$ ratio, ignoring isotope effects in these reactions. Indeed, while the $k_{CH_{3+}}=1.1\times10^{-9}\,cm^3\,s^{-1}$ ($k_{CH_{2+}}=3.9\times10^{-9}\,cm^3\,s^{-1}$)[17] rate constants for the reactions between CH_3^+ (CH_2^+) and CH_4 are reasonably known,[17–19] this is not the case for the reactions of CD_3^+ or CD_2^+ with CD_4.[18,20] We used the same ratio at all collision energies. This assumes first that secondary reactions are independent of collision energy. There is no doubt that this assumption can induce a bigger error than the one due to the isotope effect. For the $N_2^+ + CH_4$ system, the situation is worse because of the mass overlap between N_2H^+ and $C_2H_5^+$. The contribution of $C_2H_5^+$ ions to mass 29 is determined from the ratio between the intensities of $C_2D_5^+$ ions (mass 34) and N_2D^+ ions (mass 30). Again, we neglected the isotope effect. This assumption increases the error on the integral cross sec-

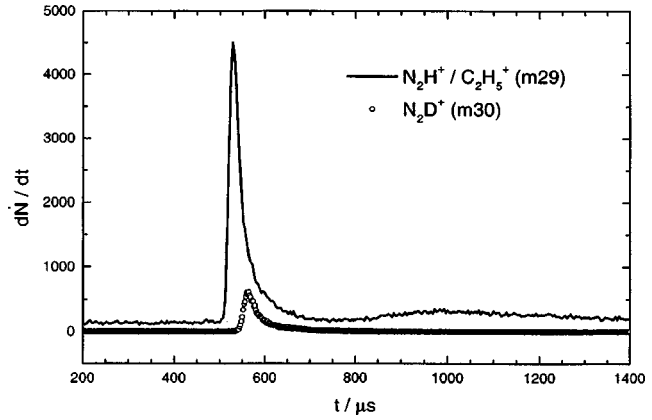

FIG. 1. N_2H^+ and N_2D^+ product ion time-of-flight (TOF) distributions recorded at 1 eV collision energy. The solid line corresponds to mass 29 u, i.e., N_2H^+ (peak around 528 μs) and $C_2H_5^+$ (background plus wide peak at longer arrival times) in the $N_2^+ + CH_4$. The open circles correspond to N_2D^+ ions produced in $N_2^+ + CD_4$ collisions.

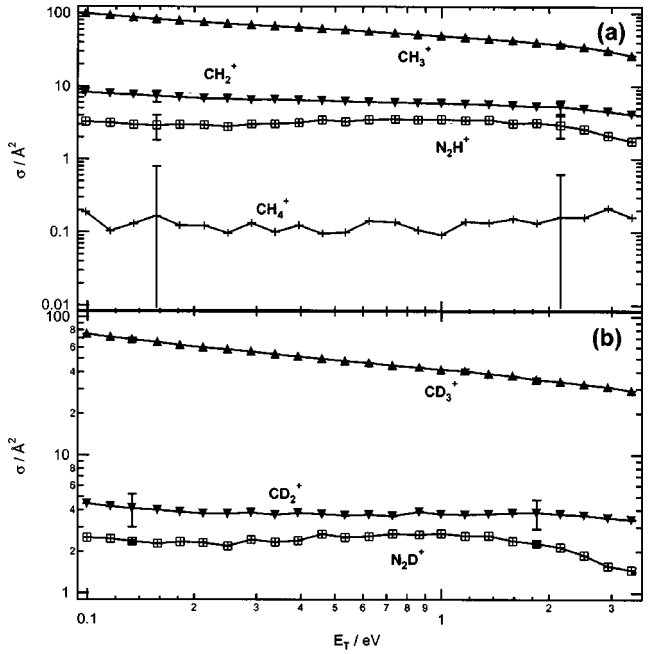

FIG. 2. Absolute integral cross sections as a function of collision energy for the products of the $N_2^+ + CH_4$ (a) and $N_2^+ + CD_4$ (b) systems. The results are corrected for secondary reactions.

tion of the (4H) channel. It is, however, important to note that the CH_3^+/CH_2^+ and CD_3^+/CD_2^+ ratios are not affected by these corrections over the whole collision energy range (see below).

B. Differential cross section

In order to precisely ($\pm$5 meV) calibrate the kinetic energy of the primary ions using time-of-flight (TOF) and to determine arrival times of the product ions, the primary ion beam is pulsed. The TOF distributions are recorded by a multichannel scaler with a dwell time of 4 μs. Figure 1 shows two TOF distributions measured at 1 eV collision energy for product ions with mass 29. The pronounced peak at 528 μs corresponds to the N_2H^+ primary product and the background plus the wide peak at later arrival times to the isobaric $C_2H_5^+$ secondary product. These assignments can be corroborated by comparison with the N_2D^+TOF spectrum (open circles), where there is no mass overlap and only one peak at 560 μs. Due to the special GIB scattering geometry, single differential cross sections with respect to the axial velocity, $d\sigma/du'_{1p}$, can already provide important information about the reaction mechanism. The determination of the transverse velocity component, u'_{1t}, is also possible by varying the amplitude of the rf guiding field (GIB-VAR method). For a detailed discussion including the numerical procedure and the influence of the target motion, see Refs. 13, 21. The fit of the velocity distribution by the combination of two Gaussian functions, in order to determine the $\langle u'_{1p} \rangle$ mean product velocity is justified and explained in Ref. 13. In the following, the unprimed symbols refer to the ionic and neutral reactants, the primed symbols to the products.

IV. RESULTS

A. Absolute integral cross sections

The corrected absolute integral cross sections for the two systems are shown in Figs. 2(a) and 2(b), respectively. Table I presents the corrected (in bold) and the uncorrected (between brackets) absolute integral cross sections for all channels at four selected collision energies. Sum cross sections for the two systems are also reported in Table I. All product channels for the CH_4 target gas have a cross section bigger than their deuterated equivalents. The dominant product channel is the (2H) dissociative charge transfer channel leading to CH_3^+ ions. It also produces molecular nitrogen and atomic hydrogen. All other channels contribute with less than 15%. The reactive cross section for nondissociative charge transfer is estimated from the mass 16 u signal that is dominated by $^{13}CH_3^+$. The integral cross section for this channel is below 0.1 Å^2. The channel leading to CD_4^+ is not reported, because its mass overlaps with ND_3^+ and H_2DO^+. The absolute reactive cross section of $CH_3^+(CD_3^+)$ decreases with collision energy from 99 Å^2 (75 Å^2) to 31 Å^2. For the CH_2^+ channel, the absolute reactive cross section decreases from 8 to 6 Å^2 with increasing collision energy, whereas the CD_2^+ channel displays a constant value of 4 Å^2. The absolute reactive cross section for N_2D^+ is constant at collision energies between 0.1 and 0.3 eV and decays slowly above 1 eV.

Table II summarizes the CH_3^+ and CH_2^+ percentages averaged over the investigated collision energy range obtained before and after the secondary reaction corrections. These values are compared with the literature values,[5,6] as well as the values obtained for the $Ar^+ + CH_4$ reaction (see the discussion). The last line of Table II contains the photon energy for which the dissociative photoionization of methane gives the same CH_3^+ and CH_2^+ percentages[22] (see the discussion). The CH_3^+ and CH_2^+ branching measured in this study are in very good agreement with previous studies.[5,6] The almost constant ratio over the collision energy range is also in good agreement with previous observations, indicating that the temperature may have only a minor effect on this ratio.[7] The percentages obtained for the $N_2^+ + CD_4$ system (92$\pm$2% CD_3^+ and 8$\pm$2% CD_2^+) and the $N_2^+ + CH_4$ system are similar.

TABLE I. Absolute integral cross sections in Å^2 obtained in this work for four different collision energies. The bold numbers and numbers between brackets are the absolute integral cross sections that are corrected and not corrected from secondary reactions, respectively.

Product ions	Collision energy			
	0.1 eV	0.3 eV	1 eV	3 eV
CH_4^+	**0.2**	**0.1**	**0.1**	**0.2**
CH_3^+	**99.1** (84.7)	**68.9** (58.1)	**48.6** (39.8)	**30.7** (23.7)
CH_2^+	**8.3** (7.8)	**6.5** (6.1)	**5.9** (5.4)	**4.5** (9.5)
$N_2H^-(N_2H^+/C_2H_5^+)$	**3.3** (18.2)	**3.0** (14.2)	**3.5** (12.7)	**2.1** (4.1)
SUM	**110.9**	**78.5**	**58.1**	**37.5**
CD_3^+	**75.0** (63.8)	**56.0** (47.2)	**41.4** (34.6)	**31.1** (25.8)
$C_2D_5^+$	−(11.5)	−(9.0)	−(7.1)	−(5.6)
CD_2^+	**4.6** (4.2)	**3.8** (3.6)	**3.7** (3.5)	**3.5** (3.3)
N_2D^+	**2.5**	**2.4**	**2.7**	**1.6**
SUM	**93.6**	**71.2**	**54.9**	**41.8**

B. Differential cross sections

Figures 3–5 show velocity distributions of the indicated protonated (left column) and deuterated (right column) product ions at selected collision energies between 0.10 and 3.5 eV. Laboratory (v'_{1p}) and center-of-mass (u'_{1p}) velocities, in $10^4\,\mathrm{ms}^{-1}$, are represented on the bottom axis in the usual way, as described in Ref. 13. The product laboratory energy is denoted E'_{1p}. The top axis represents the product center of mass energy, E'_T, which is calculated from the measured velocity component u'_{1p}, i.e., assuming that the transverse velocity component of the product ion, u'_{1t}, is negligible. If products are predominantly forward or backward scattered, this assumption is often fulfilled. However, if ions are sideward scattered, the GIB-VAR method has to be used. The second assumption made to calculate this axis is that the reaction produces only one ion and one neutral molecule. This is not the case for (2H–D) and (3H–D) channels, so this scale is only valid if one makes special assumptions concerning the decay into the three-body system. The dashed line represents the center of mass velocity, v_{CM}, of the collision system. The two dash–dotted lines are the product laboratory velocities for those reactions where E'_T is equal to E_T, i.e., there is no conversion of internal energy into translational energy, and *vice versa*.

With increasing collision energy, the intensity at very low laboratory velocities rises. This, however, does not correspond to subthermal energies but is in reality due to an accumulation of ions with very long flight or residence times. These ions are either backward scattered or trapped by potential distortions in the first octopole.

The axial velocity distributions shown in Figs. 3 and 4 clearly reveal that the CH_2^+ and CH_3^+ product ions and deu-

TABLE II. Averaged percentages over the investigated collision energy range of CH_3^+ and CH_2^+ ions, obtained in this work before and after the secondary reaction corrections. (a) Ref. 6; (b) Ref. 5; (c) Ref. 26; (d) Ref. 25; (e) photon energy for which the dissociative photoionization of methane gives the same percentages (Ref. 22).

Product ions	N_2^+(IP 15.58 eV) + CH_4				Ar^+(15.76 eV) + CH_4	
	Present data		Literature		Literature	
	Not corrected	Corrected	(a)	(b)	(c)	(d)
CH_3^+	89±2%	90±2%	89%	93%	85±3%	85±1%
CH_2^+	11±2%	10±2%	11%	7%	15±3%	15±1%
$h\nu$ (eV)(e)	15.3	15.3	⋯	⋯	15.3	15.3

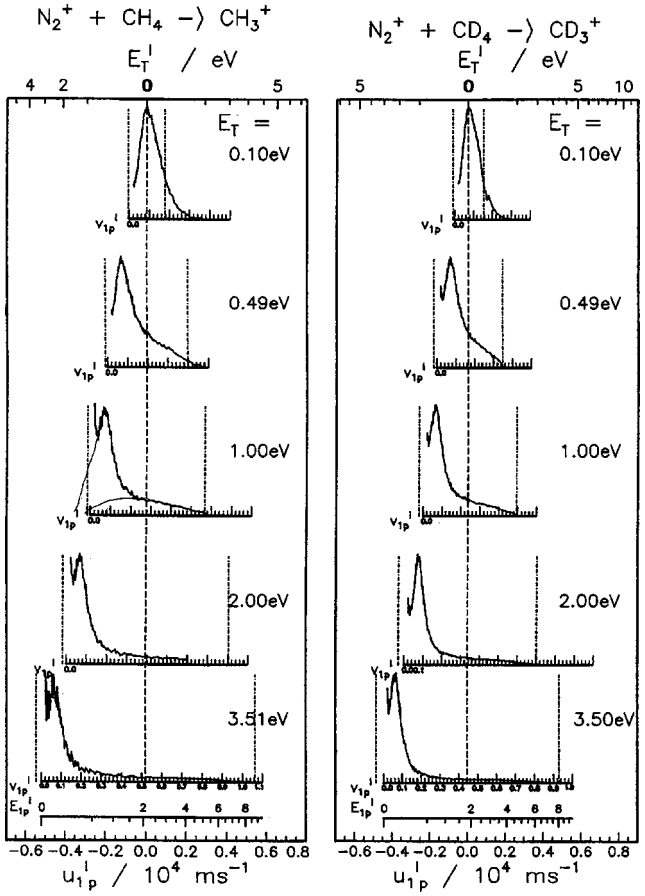

FIG. 3. Axial velocity distributions for CH_3^+ and CD_3^+ product ions. Laboratory (v'_{1p}) and center-of-mass (u'_{1p}) velocities (in $10^4\,\mathrm{ms}^{-1}$), as well as laboratory energy (E'_{1p}) of the products (in eV) are represented on the bottom axis. On the top axis, there is the corresponding center-of-mass product energy in (E'_T). The dashed line in the middle is v_{CM} and the two dash–dotted lines are the product laboratory velocities for the maximum positive and negative product velocities in the center-of-mass, assuming that E_T and E'_T are equal (see the text).

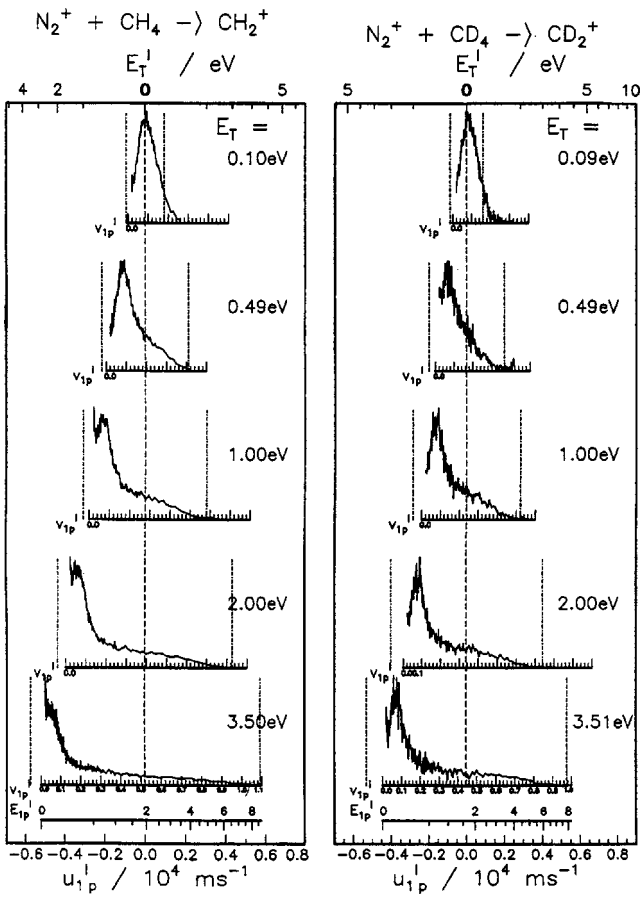

FIG. 4. Axial velocity distributions for CH_2^+ and CD_2^+ product ions. Concerning the scales see Fig. 3.

terated analogs are all very slow in the laboratory frame. As can be seen in these figures, the product velocity distributions for forming CH_3^+ and CH_2^+ is symmetric around the center of mass velocity at 0.1 eV. At and above 0.49 eV the distributions clearly exhibit two components, a main peak the location of which corresponds, with increasing collision energy, more and more to backward scattered ions, and a broad peak that looks symmetric around the center-of-mass. The latter decreases in intensity with collision energy.

Above 0.1 eV collision energy, the $N_2H^+/C_2H_5^+$ velocity distribution shows two well-separated peaks, one backward scattered and the other one forward scattered. The comparison with the velocity distribution of N_2D^+ allows a clear assignment of the forward peak to N_2H^+ ions. The velocity distribution of N_2H^+ and N_2D^+ are more and more forward scattered with increasing collision energy. At 0.10 eV collision energy, because of the overlap between the two N_2H^+ and $C_2H_5^+$ peaks, the forward and backward components can no longer be separated. Note also that for collision energies higher than 1 eV, the forward scattered velocity distribution is narrower for the deuterated product. The fact that the distribution of the protanated product is broader cannot be due to some perturbation caused by $C_2H_5^+$ secondary products because, at these collision energies, the two contributions are well separated.

V. DISCUSSION

A. Charge transfer and dissociative charge transfer channels

The cross section for the nondissociative charge transfer channel is very small (<0.1 Å^2), even at the lowest collision energy. This means that a substantial part of the 2.97 eV reaction exothermicity goes into CH_4^+ internal energy, at least an amount larger than the dissociation energy of 1.64 eV.[23] It is interesting to compare the results of this paper with the Ar^+[24,25] (and references therein) and Kr^+[26–28] reactions with methane. Argon and nitrogen have very close ionization potentials (15.76 and 15.58 eV, respectively), whereas Kr has a much lower IP (14.00 eV). As expected from the energetics, CH_4^+ products are observed only from the Kr^+ reaction with methane.

At $E_T = 0.1$ eV, the $CH_3^+ : CH_2^+ : N_2H^+$ branching ratio is 0.90:0.07:0.03 and does not vary significantly with collision energy. This result differs from the thermal ratio found by McEwan *et al.* (0.80:0.05:0.15).[1] This discrepancy cannot be explained by the difference in collision energy, because it is unlikely that there is a sudden change if the collision energy increases for thermal energies to 0.1 eV. Most probably, the value reported by McEwan *et al.* has not been corrected for secondary reactions. This ratio, averaged over the whole range of collision energy, is 0.86:0.09:0.05 for the $N_2^+ + CH_4$ system and 0.88:0.07:0.05 for the $N_2^+ + CD_4$ system.

Reactions of N_2^+ and Ar^+ with methane give almost exactly the same CH_3^+/CH_2^+ ratio (see Table II), even though the dissociation of CH_4^+ strongly varies with its internal energy.[22] This indicates that both reactions involve a similar dissociative charge transfer mechanism.

The reactions (2) and (3) may both proceed via a separated sequential process, i.e., that there is first an impulsive single-electron transfer, and then, later, the methane ion dissociates. The independence of the CH_3^+/CH_2^+ ratio on the collision energy range indicates that kinetic energy is not converted efficiently into internal energy of the methane ion. Assuming that the measured CH_3^+/CH_2^+ ratio is only determined by the internal energy, one can deduce the internal energy of the produced CH_4^+ ions by comparing the branching ratio with those measured in dissociative photoionization experiments. This assumption is based on the fact that Franck–Condon (FC) principles could be also applied to a resonant charge transfer process occurring at long range distances. If FC factors favor the transition between ground vibrational states of nitrogen, it is not the case for methane, the ion and neutral having different geometries. The photon energy that leads to the same CH_3^+/CH_2^+ ratio in the dissociative photoionization of methane is 15.3 eV.[22] This value is lower than the N_2^+ recombination energy, so the charge transfer is not completely resonant. However, first charge transfer results in an internal energy distribution (which may be fairly narrow in a ''quasiresonant'' system as the present one), unlike a monochromatic photoionization experiment. Second, the vibrational motion cannot be assumed to be frozen in low-energy charge transfer collisions, as is the case in the photoionization experiments. With this value of 15.3 eV, the internal energy of the $(CH_4^+)^*$ produced in the charge trans-

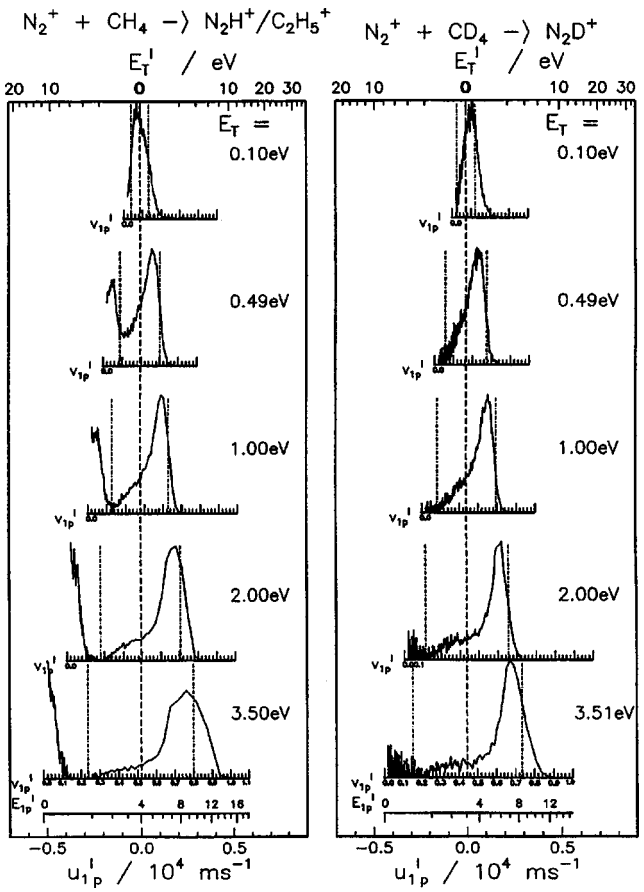

FIG. 5. Axial velocity distributions for mass 29 ($N_2H^+/C_2H_5^+$) and mass 30 (N_2D^+) product ions. Concerning the scales, see Fig. 3.

fer from N_2^+ is equal to 2.7 eV, i.e., the difference between 15.3 and 12.61 eV [IP(CH_4)]. In the dissociation, due to the mass ratio between the products, most of the energy is carried away by the H(H_2) neutral product. Therefore the (2H) and (3H) channels are also sources of production of energetic H_2 and H neutrals. This certainly affects the reactivity of these species and should be taken into account in the ionospheric models. The main peak of velocity distributions, for the CH_3^+ and CH_2^+ ions, most probably reflects a distribution both in rotational excitation and deflection angle of these products, as momentum is transferred during the charge transfer. In these velocity distributions, there is another component, which looks symmetric relative to the center of mass velocity. It indicates that part of the dissociative charge transfer involves an intermediate complex that is long lived in comparison to a rotational period. At low collision energies, it represents a substantial part of the charge transfer channels and decreases with collision energy, as expected for such a mechanism. However, more experimental work would be necessary to fully understand this process. In summary, the dissociative charge transfer involves two different reaction mechanisms: the main one is a charge transfer with some momentum transfer and the second one involves a long-lived intermediate complex.

Figure 6 shows the sum of the cross sections for all reactive channels versus collision energy for the reaction with CH_4, as well as the CH_3^+ production cross section and

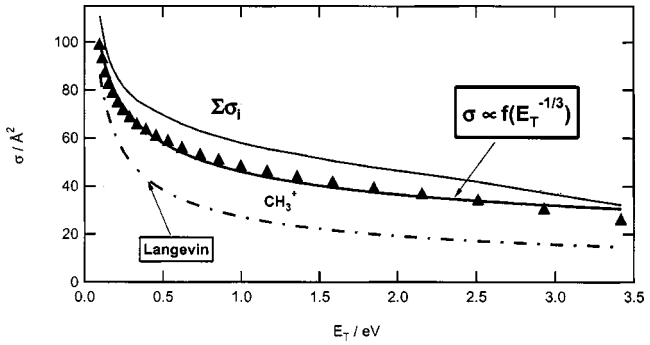

FIG. 6. The sum of the cross section (full line) for all reactive channels and absolute integral cross section for CH_3^+ (triangles) vs collision energy. The dash-dotted line is the Langevin cross section. The line going through the triangles shows a decrease of the $\sigma \propto E_T^{-1/3}$ type.

the Langevin cross section. At thermal collision energy, the sum cross section, which is mainly due to the (2H) channel giving CH_3^+ ions, is very close to the Langevin model, but its decrease with collision energy is much slower than the Lanvegin one. This has also been observed for the charge transfer between the Kr cations and Ar cations and methane. The theoretical model developed for the $Kr^+ + CH_4$ reaction and based on a quasiresonant charge-exchange mechanism ($\sigma \propto E_T^{-1/3}$) fits well the experimental CH_3^+ cross section dependence with collision energy.[26] The dependence of the rate coefficient with temperature has also been shown to be weak.[7,29]

The magnitude of the total cross section indicates, as for the $Ar^+ + CH_4$ reaction,[25] an efficient nonadiabatic coupling between the two charge-states, $N_2^+ + CH_4$ and $CH_4^+ + N_2$, with a large probability when the first relevant crossing is reached. The fact that the ratio CH_3^+/CH_2^+ does not depend on collision energy confirms this strong coupling. If this were not the case, the successive crossings reached by increasing the collision energy would most probably produce a different product branching ratio. As almost the same energy is transferred to $(CH_4^+)^*$ in both reactions, with a little more energy in the case of the more energetic argon ion, we assume that the potential energy surfaces for $Ar^+ + CH_4$ and $N_2^+ + CH_4$ are similar. The crossing may occur at a slightly longer $N_2 - CH_4$ internuclear distance than for the argon system. But it cannot be at a very long distance, because some momentum transfer to $(CH_4^+)^*$ is measured in the distribution velocities.

B. The H transfer channel

As can be seen from Fig. 5, even at the lowest collision energy, $E_T = 0.10$ eV, the distribution velocity is not symmetric around the center of mass velocity. For N_2D^+ ions, the distribution is clearly forward peaked. This is a strong indication that the H (D) transfer occurs via a direct process. In the $N_2^+ + CH_4$ system, the backward scattered $C_2H_5^+$ contribution is explained by secondary reactions between CH_3^+ primary products with thermal CH_4, which give $C_2H_5^+$ ions with thermal laboratory velocity. A forward velocity distribution for N_2D^+ and N_2H^+ was also observed by Wyatt *et al.*[9] in the 0.65–35 eV collision energy range and at higher col-

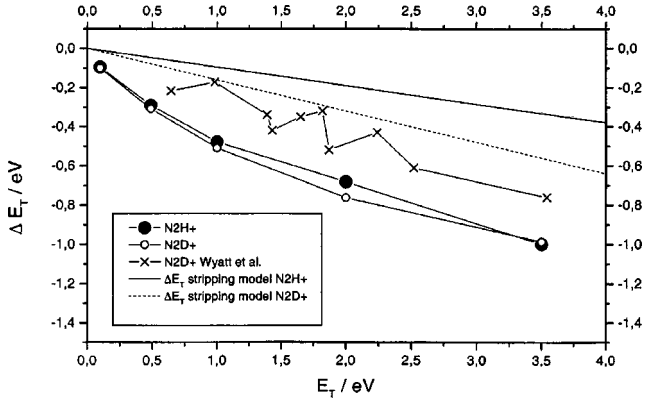

FIG. 7. Translational exoergicity ΔE_T vs collision energy. The results of the present work have been derived from the axial velocity distribution alone. This may explain why they are below the experimental values (crosses) of Wyatt *et al.* (Ref. 9). The full (dashed) line is the curve calculated with the spectator stripping model for $N_2H^+(N_2D^+)$ product ions.

lision energy (above 25 eV) by Gislason *et al.*[8] Moreover, the results of Gislason *et al.* in a crossed beam apparatus also observed a forward scattered peak in the product angular distribution, with some symmetric wings on each side of the 0° axis. This might explain a part of the width of the distribution of the velocity projection measured in this work. However, the broad distribution around the center of mass velocity is more likely due to a mechanism involving an intermediate complex, probably of the type of a capture complex, as discussed for the H transfer in the $C_2H_2^+ + CH_4$ reaction, but less pronounced.[30]

Figure 7 shows the ΔE_T difference between the energy derived from the measured mean axial velocity of the ion products and the collision energy of the parent ions. The full (dashed) line is the curve calculated with the spectator stripping model for $N_2H^+(N_2D^+)$ product ions. The ΔE_T values of this work are below the experimental ones given by Wyatt *et al.* (crosses).[9] This may be due to the kinetic energy of the transverse motion that is not measured by the GIB-TOF method alone. Both experimental values deviate somewhat from the spectator stripping model. Moreover, this model predicts an isotope effect favoring the D transfer versus the H transfer. Apparently the experimental results do not show a pronounced isotope effect.

The absolute reactive cross sections show the same isotope effect favoring the abstraction of H versus D as the one found by Wyatt *et al.*[9] But no threshold in the reaction for channels (4H–D) at $E_T = 0.1$ eV is found.[9] The reactive cross sections measured by these authors are ten times smaller than our results and the one obtained at higher collision energy by Gislason *et al.*[8] Let us note that the H transfer channel represents about 5% of the total cross section, whereas it is negligible in the case of the $Ar^+ + CH_4$ reaction.[31] This difference may be explained by the higher proton affinity of N_2 (493.8 kJ/mol) compared with the Ar one (369.2 kJ/mol).

VI. CONCLUSION

Absolute integral cross sections and product branching ratios have been measured as a function of collision energy between 0.1–3.5 eV in the center of mass frame for the $N_2^+ + CH_4$ and $N_2^+ + CD_4$ reactions. The previously reported values for the branching ratio are most probably affected by secondary collisions.[1] In order to correct the present measurements, we used the deuterated system for which there is no mass overlap between N_2D^+ ion products and $C_2D_5^+$ ions coming from secondary collisions. Further experiments with isotopic $^{15}N_2$ could simplify the data treatment by cancelling the mass overlaps in the $N_2^+ + CH_4$ system.

The dominant reaction channels are the dissociative charge transfer and the H (D) atom transfer, the nondissociative charge transfer being negligible. Almost no isotope effect is observed for the reaction branching ratio, which strongly favors the $CH_3^+(CD_3^+)$ ion production. However, the absolute cross sections are larger for the $N_2^+ + CH_4$ system compared to those of the $N_2^+ + CD_4$ system. The magnitude of the total cross section suggests an efficient nonadiabatic coupling between the two nonresonant charge transfer states, $N_2^+ + CH_4$ and $CH_4^+ + N_2$. The CH_3^+/CH_2^+ ratio measured for the $N_2^+ + CH_4$ reaction is independent of collision energy and very similar to the one obtained for the $Ar^+ + CH_4$ reaction. By comparing this ratio with the breakdown curve of dissociative photoionization of methane, it is concluded that CH_4^+ is first produced by charge transfer with an internal energy equal to 2.7 eV.

Axial velocity distributions of the products at different collision energies between 0.1 and 3.5 eV CM, have been recorded for all channels of the two systems. They give a direct insight into the elementary reaction dynamics. The dissociative charge transfer occurs via a charge transfer process with some momentum transfer followed by CH_4^+ dissociation. A similar mechanism was proposed for the $Ar^+ + CH_4$ reaction.[25] A noticeable difference is that the H (D) transfer channel is negligible for the $Ar^+ + CH_4$ reaction. This is most probably due to the difference in proton affinities between N_2 and Ar. The forward peaked velocity distribution of $N_2H^+(N_2D^+)$ ions clearly shows that the H (D) transfer occurs via a direct process, as previously reported.[9] However, both the maximum of the distribution and its broadness indicate that it does not completely follow a spectator stripping mechanism.

The present reliable branching ratio for the $N_2^+ + CH_4$ reaction should now be used in the Titan ionosphere modeling, due to its importance as one of the first steps in the chemistry of this atmosphere. Moreover, the production of "hot" H and H_2 neutrals (temperatures higher than 3000 K) should also be taken into account in those models even though H and H_2 are minor constituents in Titan's ionosphere.[32]

The present work would deserve theoretical studies and further experimental work, in particular concerning the angular distribution of product ions, in order to get a more precise insight into the reaction dynamics. Theoretical calculations of potential energy surfaces could, in particular, help for localizing the crossing point of the curves, leading to a better understanding of the dissociative charge transfer.

ACKNOWLEDGMENTS

This work was generously supported by the VW foundation within the program *Intra-und Intermolekulare*

Elektronenübertragung (I/69959) and by the TMR network Astrophysical Chemistry under Contract No. ERB FMRX-CT97-0132.

[1] M. J. McEwan, G. B. I. Scott, and V. G. Anicich, Int. J. Mass Spectrom. Ion Phys. **178**, 209 (1998).
[2] C. N. Keller, T. E. Cravens, and L. Gan, J. Geophys. Res. **97**, 12117 (1992).
[3] C. Nicolas, C. Alcaraz, R. Thissen, Z. Zabka, and O. Dutuit, Planet. Space Sci. **50**, 877 (2002).
[4] J. Gauglhoffer and L. Kevan, Chem. Phys. Lett. **16**, 492 (1972); P. Ausloos, J. R. Eyler, and S. G. Lias, *ibid.* **30**, 21 (1975).
[5] M. Tichy, A. B. Raskshit, D. G. Lister, N. D. Twiddy, N. G. Adams, and D. Smith, Int. J. Mass Spectrom. Ion Phys. **29**, 231 (1979).
[6] D. Smith, N. G. Adams, and T. M. Miller, J. Chem. Phys. **69**, 308 (1978).
[7] L. K. Randeniya and M. A. Smith, J. Chem. Phys. **94**, 351 (1991).
[8] E. A. Gislason, B. H. Mahan, C. Tsao, and A. S. Werner, J. Chem. Phys. **50**, 142 (1969).
[9] J. R. Wyatt, L. W. Strattan, S. C. Snyder, and P. M. Hierl, J. Chem. Phys. **64**, 3757 (1976).
[10] J. Glosik, A. Luca, S. Mark, and D. Gerlich, J. Chem. Phys. **112**, 7011 (2000).
[11] S. H. Pullins, R. A. Dressler, R. Torrents, and D. Gerlich, Z. Phys. Chem. (Munich) **214**, 1279 (2000).
[12] E. Haufler, S. Schlemmer, and D. Gerlich, J. Phys. Chem. **101**, 6441 (1997).
[13] S. Mark and D. Gerlich, Chem. Phys. **209**, 235 (1996).
[14] R. H. Schultz and P. B. Armentrout, Chem. Phys. Lett. **179**, 429 (1991).
[15] W. Lindinger, F. Howorka, P. Lukac, S. Kuhn, H. Villinger, E. Alge, and H. Ramler, Phys. Rev. A **23**, 2327 (1981).
[16] R. Torrents, Ph.D. thesis, Technical University Chemnitz, 2001
[17] V. G. Anicich and M. J. McEwan, Planet. Space Sci. **45**, 897 (1997).
[18] L. W. Sieck and S. G. Lias, J. Phys. Chem. Ref. Data **5**, 1123 (1976).
[19] N. G. Adams and D. Smith, Chem. Phys. Lett. **47**, 383 (1977).
[20] R. A. Fluegge and D. A. Landman, J. Chem. Phys. **54**, 1576 (1971).
[21] D. Gerlich, J. Chem. Phys. **90**, 127 (1989).
[22] R. Stockbauer, J. Chem. Phys. **58**, 3800 (1973).
[23] S. G. Lias, J. F. Bartmess, J. F. Liebman, J. L. Holmes, R. D. Levin, and W. G. Mallard, J. Phys. Chem. Ref. Data, Suppl. **17**, 1 (1988).
[24] M. Tsuji, H. Kouno, K. Matsumura, and T. Funatsu, J. Chem. Phys. **98**, 2011 (1993).
[25] P. Tosi, D. Cappelletti, O. Dmitriev, S. Giordani, D. Bassi, D. R. Latimer, and M. A. Smith, J. Phys. Chem. **99**, 15538 (1995).
[26] P. Tosi, C. Delvai, D. Bassi, O. Dmitriev, D. Cappelletti, and F. Vecchiocattivi, Chem. Phys. **209**, 227 (1996).
[27] Z. Herman and B. Friedrich, J. Chem. Phys. **102**, 7017 (1995).
[28] Z. Herman, K. Birkinshaw, and V. Pacak, Int. J. Mass Spectrom. Ion Processes **135**, 47 (1994).
[29] B. R. Rowe, J. B. Marquette, and C. Rebrion, J. Chem. Soc., Faraday Trans. 2 **85**, 1631 (1989).
[30] J. Zabka, O. Dutuit, Z. Dolejsek, J. Polach, and Z. Herman, Chem. Phys. **2**, 781 (2000).
[31] M. Hawley and M. A. Smith, J. Phys. Chem. **96**, 6693 (1992).
[32] D. Toutblanc, J. P. Brillet, D. Gautier, F. Raulin, and C. P. McKay, Icarus **113**, 2 (1995).